Temperature-Controlled Structure and Kinetics of Ripple Phases in One- and Two-Component Supported Lipid Bilayers

Thomas Kaasgaard,* Chad Leidy,* John H. Crowe,† Ole G. Mouritsen,‡ and Kent Jørgensen*
*Department of Chemistry, Technical University of Denmark, Lyngby, Denmark; †Section of Molecular and Cellular Biology, University of California, Davis, California USA; and ‡MEMPHYS-Center for Biomembrane Physics, Department of Physics, University of Southern Denmark, Odense, Denmark T. Kaasgaard and C. Leidy contributed equally to this work.

ABSTRACT Temperature-controlled atomic force microscopy (AFM) has been used to visualize and study the structure and kinetics of ripple phases in one-component dipalmitoylphosphatidylcholine (DPPC) and two-component dimyristoylphosphatidylcholine-distearoylphosphatidylcholine (DMPC-DSPC) lipid bilayers. The lipid bilayers are mica-supported double bilayers in which ripple-phase formation occurs in the top bilayer. In one-component DPPC lipid bilayers, the stable and metastable ripple phases were observed. In addition, a third ripple structure with approximately twice the wavelength of the metastable ripples was seen. From height profiles of the AFM images, estimates of the amplitudes of the different ripple phases are reported. To elucidate the processes of ripple formation and disappearance, a ripple-phase DPPC lipid bilayer was taken through the pretransition in the cooling and the heating direction and the disappearance and formation of ripples was visualized. It was found that both the disappearance and formation of ripples take place virtually one ripple at a time, thereby demonstrating the highly anisotropic nature of the ripple phase. Furthermore, when a two-component DMPC-DSPC mixture was heated from the ripple phase and into the ripple-phase/fluid-phase coexistence temperature region, the AFM images revealed that several dynamic properties of the ripple phase are important for the melting behavior of the lipid mixture. Onset of melting is observed at grain boundaries between different ripple types and different ripple orientations, and the longer-wavelength metastable ripple phase melts before the shorter-wavelength stable ripple phase. Moreover, it was observed that the ripple phase favors domain growth along the ripple direction and is responsible for creating straight-edged domains with 60° and 120° angles, as reported previously.

INTRODUCTION

Lipid bilayers can exist in a variety of different phases, depending on temperature and composition. One of the more intriguing phases is the ripple phase, which is characterized by corrugations in the lipid bilayer with a well-defined periodicity. The ripple phase exists in a temperature range between the pretransition temperature and the main phase transition temperature and is observed only for certain lipid families. The molecular origin of ripple-phase formation has traditionally been associated with the lipid headgroup region, and for this reason lipids are normally divided into ripple-forming lipids and non-ripple-forming lipids based on their headgroups. One of the families of ripple-forming lipids is the extensively studied phosphatidylcholines (Lewis et al., 1987).

Several attempts have been made to explain why ripple phases form. Numerous models share the common idea that ripples result from a periodic local spontaneous curvature in the lipid bilayer. Many different reasons for the origin of this local spontaneous curvature have been suggested, including electrostatic coupling between water molecules and the polar lipid headgroups (Doniach, 1979), coupling between membrane curvature and molecular tilt (Lubensky and Mackintosh, 1993), and generation of curvature by linear arrays of fluid state lipid molecules (Heimburg, 2000). Other models assume that ripples form to relieve packing frustrations that arise whenever the relationship between headgroup cross-sectional area and the cross-sectional area of the apolar tails exceeds a certain threshold (Carlson and Sethna, 1987; Kirchner and Cevc, 1994).

The ripple phase has been extensively studied by a variety of experimental techniques. Freeze-fracture electron microscopy studies have visualized the structure of ripple phases as periodic linear arrays of ripples, which at certain points change direction by characteristic angles of 60° or 120° (Fluck et al., 1969; Ververgaert et al., 1973; Copeland and McConnell, 1980; Rüppel and Sackmann, 1983; Meyer, 1996). These angles are most likely a reflection of the hexagonal packing of the lipids. In phosphatidylcholine bilayers, two different ripple structures form—a stable one and a metastable one, depending on the thermal history of the sample (Zasadzinski, 1988; Tenchov et al., 1989; Tenchov, 1991; Yao et al., 1991; Koynova et al., 1996; Katsaras et al., 2000). The stable ripple phase forms at the pretransition temperature upon heating from the gel phase. It has an asymmetric sawtooth profile, and the acyl chains are tilted with respect to the bilayer normal. The metastable ripple phase forms at the main phase transition upon cooling from the fluid phase and has approximately double the ripple repeat distance of the stable ripple phase. The metastable ripple phase has a symmetric profile and the acyl chains are oriented parallel to the bilayer normal. The ripple repeat distance is ~130–150 Å and 260–300 Å for the stable and metastable ripples, respectively, and is slightly dependent on

Submitted January 21, 2003, and accepted for publication March 7, 2003.

T. Kaasgaard and C. Leidy contributed equally to this work.

Address reprint requests to K. Jørgensen, Dept. of Chemistry, Bldg. 206, Technical University of Denmark, DK-2800 Lyngby, Denmark. Fax: 45-4-588-3136; E-mail: jorgense@kemi.dtu.dk.

0006-3495/03/07/350/11 $2.00

both the temperature (Mortensen et al., 1988; Matuoka et al., 1994) and the lipid species (Hicks et al., 1987). Because of the tendency of the ripple wavelength to approximately double in size, the stable ripples have been denoted Λ/2-ripples and the metastable ripples Λ-ripples. We shall adopt this nomenclature in the present article.

The exact structure of the ripple phase has also been subject to considerable debate. Janiak et al. (1979) proposed that the lipid molecules are organized in a two-dimensional hexagonal lattice on which the periodic ripple modulation is superimposed. The ripple periodicity in the Λ/2-ripple phase corresponds to ~20 lipid molecules, illustrating that the length scale of the ripple modulation is considerably larger than the molecular length scale of the underlying hexagonal lattice. The ripple modulation distorts the hexagonal lattice of the lipids. This has the important consequence that lipid molecules, which reside in identical positions with respect to the underlying two-dimensional hexagonal lattice, experience different local environments if they reside in different positions with respect to the ripple modulation. This effect is reflected in a couple of models that assume that the variation in bilayer curvature across the ripple profile may be directly related to the phase state of the lipids (Carlson and Sethna, 1987; Heimburg, 2000). In support of these models, experimental studies have indicated coexistence of gel-state and fluid-state lipids in the ripple phase (Sun et al., 1996; Rappolt et al., 2000). Other studies, in contrast, claim that ripple phases consist almost entirely of gel-state lipid molecules (Rappolt and Rapp, 1996).

In solid supported single lipid bilayers, which are most often used for atomic force microscopy (AFM) studies, the ripple phase is not observed when standard preparation techniques are used. To our knowledge, the only reports where ripple-phase formation has been observed in supported lipid bilayers include, 1), Ripple-phase formation in asymmetric lipid bilayers prepared by Langmuir-Blodgett deposition and imaged using specific salt concentrations (Czajkowsky et al., 1995); 2), lipid bilayers imaged in tris-buffer (Mou et al., 1994); and 3), ripples in the top bilayers of supported double bilayers (Fang and Yang, 1996; Leidy et al., 2002). The observations of a rippled texture in supported double bilayers clearly indicate that studies of the ripple phase are accessible by AFM, provided that supported double bilayers are used, rather than the more traditional supported single lipid bilayers. The use of AFM to study ripple phases offers several advantages, as it allows for direct visualization of the ripple phase on the nanometer length scale in fully hydrated lipid bilayers at the relevant temperatures. Furthermore, it facilitates studies of structural changes of dynamic processes that occur on the minute timescale, which is exactly the relevant timescale for the structural rearrangements that take place at the pretransition (Tsuchida et al., 1985).

We reported in a recent article that ripple-phase domains can coexist with a fluid phase in a binary lipid mixture, and we showed that the anisotropic nature of the ripples had a significant effect on the morphology of the coexisting ripple-phase and fluid-phase domains (Leidy et al., 2002). Similar domain morphologies have been observed in giant unilamellar vesicles by fluorescence microscopy (Korlach et al., 1999; Bagatolli and Gratton, 2000). The purpose of the present article is twofold. On the one hand, we wish to give a detailed description of the ripple phase in one-component lipid bilayers using temperature-controlled atomic force microscopy. In our previous article (Leidy et al., 2002), we focused on two-component lipid bilayers, and the study by Fang and Yang (1996) was unfortunately done at temperatures below the pretransition and therefore did not show the structure of a thermodynamically stable ripple phase. A characterization by AFM of the ripple phase in one-component lipid bilayers is therefore still lacking. Moreover, in the present study we have visualized the dynamics of formation and disappearance of ripples at the pretransition. On the other hand, we also want to give a more detailed description of different events occurring in the melting process of two-component dimyristoylphosphatidylcholine-distearoylphosphatidylcholine (DMPC-DSPC) lipid bilayers responsible for the straight-edged elongated domain morphology found in the phase-coexistence region of this lipid mixture. We will show that several dynamic properties of the ripple phase, including anisotropic domain growth and grain boundary melting, play a role in determining the melting behavior of the two-component system.

MATERIALS AND METHODS

1,2-dimyristoyl-*sn*-glycero-3-phosphatidylcholine (DMPC), 1,2-dipalmitoyl-*sn*-glycero-3-phosphatidylcholine (DPPC), and 1,2-distearoyl-*sn*-glycero-3-phosphatidylcholine (DSPC) were purchased from Avanti Polar Lipids (Alabaster, AL) and used without further purification. Ruby muscovite mica was obtained from Plano W. Plannet GmbH (Wetzlar, Germany). Appropriate amounts of DMPC and DSPC were dissolved and mixed in chloroform. The samples were then dried under nitrogen gas and placed under vacuum overnight to remove the residual solvent. The dried lipids were dispersed in Milli-Q water to a final concentration of 3 mM. In the one-component DPPC samples the lipids were dispersed directly in Milli-Q water to a concentration of 3 mM. Aqueous multilamellar lipid dispersions were prepared by heating the samples to 65°C, followed by vortexing. Small unilamellar vesicles (SUVs) were prepared by sonication using a Labsonic U tip sonicator (B. Braun Biotech International, Melsungen, Germany) at 65°C for two periods of 7 min. Residual titanium was removed from the vesicle solution by centrifugation for 5 min at 2750 × *g*. The SUVs were immediately rewarmed to 65°C, and 1 ml of the vesicle suspension was added to a small home-built cell for the atomic force microscope containing a piece of freshly cleaved mica. The samples were incubated for 1 h at 24°C in the case of the DMPC-DSPC mixtures, and at 37°C in the case of the DPPC samples. The samples were then rinsed by exchanging 10 times the incubation solution with 20 mM NaCl solution, never allowing the supported bilayer to dry. Adding the warmed SUV suspension to the mica support, and allowing the sample to cool down during incubation to a temperature between the pretransition temperature and the main phase transition temperature, was generally a successful procedure for obtaining double bilayers. The mica-supported lipid bilayers were imaged in contact mode using a PicoSPM atomic force microscope (Molecular Imaging, Phoenix, AZ). Oxide-sharpened silicon nitride AFM probes (ThermoMicro-

scopes, Sunnyvale, CA) with nominal spring constants of 0.01 N/m (Figs. 1–4) and 0.02 N/m (Figs. 5–7) were used. The temperature was controlled by a commercially available Peltier sample stage for the AFM, and the temperature was measured at the sample stage at a position in close contact with, and at a distance <1 mm, from the supported lipid bilayers. After changing temperature, the AFM was equilibrated until thermal drift had stabilized (5–30 min, depending on the magnitude of the temperature change). To ensure that the force was kept minimal during scanning, the force was frequently decreased until the tip left the surface and subsequently slightly increased until just regaining contact. In general, ripples could be resolved only when the force was at an absolute minimum. Scanner hysteresis and small variations in temperature during scanning make precise statements about the scanning force difficult, since temperature fluctuations of the order of 0.01°C cause noticeable thermal bending of the gold-coated cantilevers. However, a conservative estimate of the force range would be 20–300 pN based on the nominal spring constant.

Single bilayers, double bilayers, or multiple bilayers are formed on the mica support depending on the incubation conditions. AFM was used to distinguish between these possibilities and to select for the conditions that produced double bilayers. Single bilayers were identified by similarities in domain patterns when compared with single bilayers of the same mixture and by the absence of ripples. For multiple bilayer samples, holes in the top bilayer allowed us to visualize the domain pattern in the bilayer immediately below the top bilayer. In the case of double bilayers, the bilayer immediately below presents the domain pattern observed in single bilayers, which is noticeably different from the domain pattern observed on the top bilayer. Often, the domain pattern of the lower bilayer was visible as imprints in the top bilayer of double bilayer samples (Leidy et al., 2002). Imaging was more difficult for preparations that produced more than two bilayers as the surface became very soft. However, it was possible to resolve that, starting with the second bilayer, the subsequent bilayers exhibit ripple-phase formation and similar domain patterns, which are drastically different from the domain patterns found in the first bilayer in close contact with the mica support.

The AFM images are in some cases presented as height mode images and in other cases as deflection mode images. Whereas height mode images give quantitative information about the sample topography, deflection mode images do not contain useful height information. However, deflection mode images highlight edges where drastic height changes occur, and therefore, in some instances, provided a better qualitative visualization of the ripple phases.

RESULTS AND DISCUSSION

Ripple phases in one-component DPPC lipid bilayers: relationship between ripple phases of different periodicities and amplitudes

Fig. 1 shows three different types of ripples coexisting in a DPPC-supported double bilayer at 37°C. The two predominant ripple types are the $\Lambda/2$- and the Λ-ripples, which in this DPPC sample have ripple periodicities of 150 Å and 280 Å, respectively. Changes in ripple direction with characteristic angles of 60° and 120° occur. In general, the ripple structures observed are very similar to what has previously been reported using freeze-fracture electron microscopy. These in situ AFM images thus lend support to earlier electron microscopy images and indicate that no major artifacts arise from the freeze-fracture procedure that is required for electron microscopy visualization (e.g., Hicks et al., 1987). In addition to the well-known $\Lambda/2$-ripples and Λ-ripples, a few macro-ripples, which are even larger than the Λ-ripples, are present. We often observe these macro-ripples within the Λ-ripple phase, where they are most frequently present as solitary macro-ripples. In a few instances, neighboring macro-ripples are present, and in these cases we observe that the ripple periodicity is approximately twice the value of the Λ-ripple phase. Thus, we shall denote them 2Λ-ripples in the following. Although the Λ-ripples are usually observed in large groupings, on rare occasions they are seen as just a few neighboring Λ-ripples inside the $\Lambda/2$-ripple phase. On very rare occasions we have also observed 2Λ-ripples within the $\Lambda/2$-ripple phase. Fig. 2 shows examples of these observations. An interesting effect to note in Figs. 1 and 2 is that the transition between different ripple types is commonly observed without a change in ripple orientation, which may indicate that the different ripple phases are closely related.

An estimate of the ripple amplitudes can be obtained from AFM images with corresponding height profiles such as the height profiles shown in Fig. 2. However, a precise measurement of the amplitude is not possible, since the sizes of the AFM tips (radius of curvature $\approx$20 nm according to manufacturer's specifications) are comparable to the size of the ripples. It is therefore unlikely that the tips are able to reach the bottom of the ripple valleys, leading to an underestimate of the amplitudes. This is particularly true in the case of the small $\Lambda/2$-ripples, where the underestimate of the amplitude is most pronounced, whereas the error is less for the Λ and 2Λ amplitudes. Regardless of this limitation, however, lower-limit values of the ripple amplitudes can be obtained from the AFM measurements. Inspection of several AFM images of DPPC lipid bilayers obtained under identical experimental conditions gave a range of amplitude values for the $\Lambda/2$-ripples with the largest values being 12 Å. The values for the Λ-ripples ranged from 20 Å to 50 Å, while the amplitude of the 2Λ-ripples ranged between 90 and 110 Å. Based on these measurements, we obtain an estimate of the lower-limit amplitudes of the different ripple phases in DPPC lipid bilayers at 37°C (Table 1).

It is interesting to note that the amplitude of the 2Λ-ripples is approximately twice the amplitude of the Λ-ripples. It has been suggested earlier that the Λ-ripples are constructed by combining two $\Lambda/2$-ripples (Meyer, 1996). If the same principle applies to the 2Λ-ripples, a doubling of the amplitude is expected, if indeed one 2Λ-ripple is composed of two Λ-ripples and the shape of the ripples remains the same for the different ripple types. If this hypothesis holds true, the predicted amplitude of the $\Lambda/2$-ripples would be $\sim$25 Å, which is one-half the value of the Λ-ripples and one-fourth of the 2Λ-ripple amplitude.

We emphasize that the amplitudes, particularly in the case of the $\Lambda/2$-ripple phase, should only be considered rough estimates because of the limitations related to the dimensions of the tip. Nevertheless, we find the measurements interesting because only very limited and scattered data on ripple amplitudes have been previously reported. Whereas the ripple periodicity is fairly easy to measure by electron microscopy

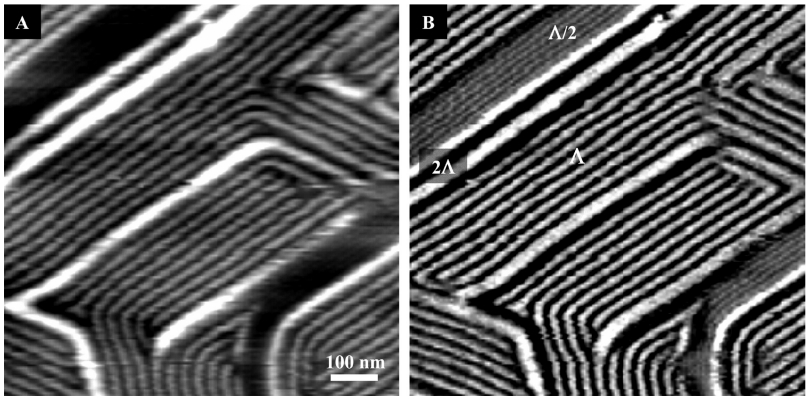

FIGURE 1 (*A*) Height mode AFM image showing different ripple phases in a DPPC-supported double bilayer at 37°C. (*B*) Deflection mode image of the same bilayer region. Three different ripple types are observed. The ripple types are denoted Λ/2-, Λ-, and 2Λ-ripples in the deflection mode image.

and x-ray diffraction, the ripple amplitude is much more difficult to assess. Scanning tunneling microscopy measurements on freeze-fractured samples have suggested that the amplitude depends strongly on temperature. It is largest just below the main phase transition, and decreases to near zero at the pretransition temperature (Woodward and Zasadzinski, 1996). In that study, the peak-to-peak ripple amplitude was reported for the Λ/2-ripple phase in DMPC lipid bilayers to be 24 Å at 23°C and 11 Å at 20°C. Other studies using scattering techniques report amplitudes of 50 Å for the Λ/2-ripple phase of DPPC at 37.5°C (Stamatoff et al., 1982) and 19 Å for DMPC lipid bilayers at an unreported temperature (Sun et al., 1996). Finally, using a technique of three-dimensional reconstruction from electron micrographs, the amplitude of DMPC ripples with a ripple repeat distance of 205 ± 30 Å was reported to be 80 Å ± 15 Å at 18°C (Krbecek et al., 1979). Most likely, this value corresponds to the Λ-ripple phase as indicated by the large amplitude and repeat distance and the ripple defect structure in the electron microscopy image (Rüppel and Sackmann, 1983).

Ripple formation and disappearance at the pretransition

Fig. 3 shows a DPPC lipid bilayer island on top of another mica-supported lipid bilayer at 37°C. At this temperature, the island consisted primarily of the metastable Λ-ripples with a few 2Λ-ripples. The sample was then cooled from 37°C to 32°C, which is just below the pretransition temperature of DPPC, and the disappearance of the ripples was monitored. In Fig. 3 *A*, which was recorded 20 min after cooling the sample, the island is still almost completely covered with ripples except for a small flat region on the right. Fig. 3, *B–D*, show how this flat region grows as more of the ripples disappear, whereas Fig. 3, *E–G*, show magnifications of different interesting events in the process of ripple disappearance, as indicated by the arrows.

In Fig. 3, *A–D*, it is clearly seen that the flat region serves as the initiation site for ripple disappearance since the flat region grows steadily with time. In addition, the arrows point to single ripples that disappear in a one-by-one manner from

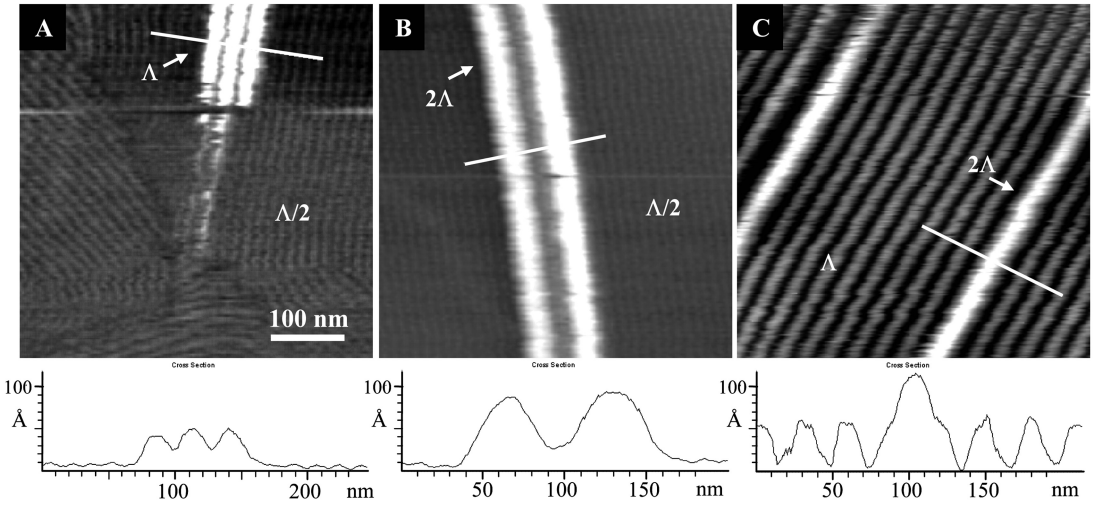

FIGURE 2 Height mode AFM images of different ripple phases. (*A*) Three neighboring Λ-ripples within the Λ/2-ripple phase. (*B*) Two neighboring 2Λ-ripples within the Λ/2-ripple phase. (*C*) Single 2Λ-ripples within the Λ-ripple phase. The height profiles corresponding to the white lines shown in the images are shown below each image.

TABLE 1 Periodicity and amplitude of different ripple phases in DPPC lipid bilayers

Ripple phase	Periodicity	Amplitude
Λ/2	150 Å	≥12 Å
Λ	280 Å	≥50 Å
2Λ	≈550 Å	≥110 Å

within the metastable Λ-ripple region. Arrow 1 in Fig. 3 *E* points to a ripple that is in the process of flattening. In the next image (Fig. 3 *F*) this ripple has disappeared completely while another ripple, arrow 2, has now partially disappeared, indicating that ripple disappearance proceeds much faster in the longitudinal direction than in the transverse direction. Arrow 3 in Fig. 3 *G* provides a particularly striking example of a single ripple, which has disappeared from within a rippled region, as this ripple makes several 60° and 120° turns.

Another interesting observation is that the disappearance of the Λ-ripples seems to take place through an intermediate conversion into the Λ/2-ripples before completely flattening (Fig. 3, *B–D*). This transition into Λ/2-ripples is another indication that the different ripple types are closely related. Fig. 3 *D* shows the lipid bilayer island after 84 min at which point the lipid bilayer consists of two flat regions surrounded by Λ/2-ripples. Because of the smaller size of the Λ/2-ripples they are not clearly visible in the height mode image. From the corresponding deflection mode image (see Fig. 4 *A*), however, it can be determined that the darker areas correspond to the flat regions whereas the brighter areas correspond to Λ/2-ripples. Interestingly, differential scanning calorimetry studies have suggested that the disappearance

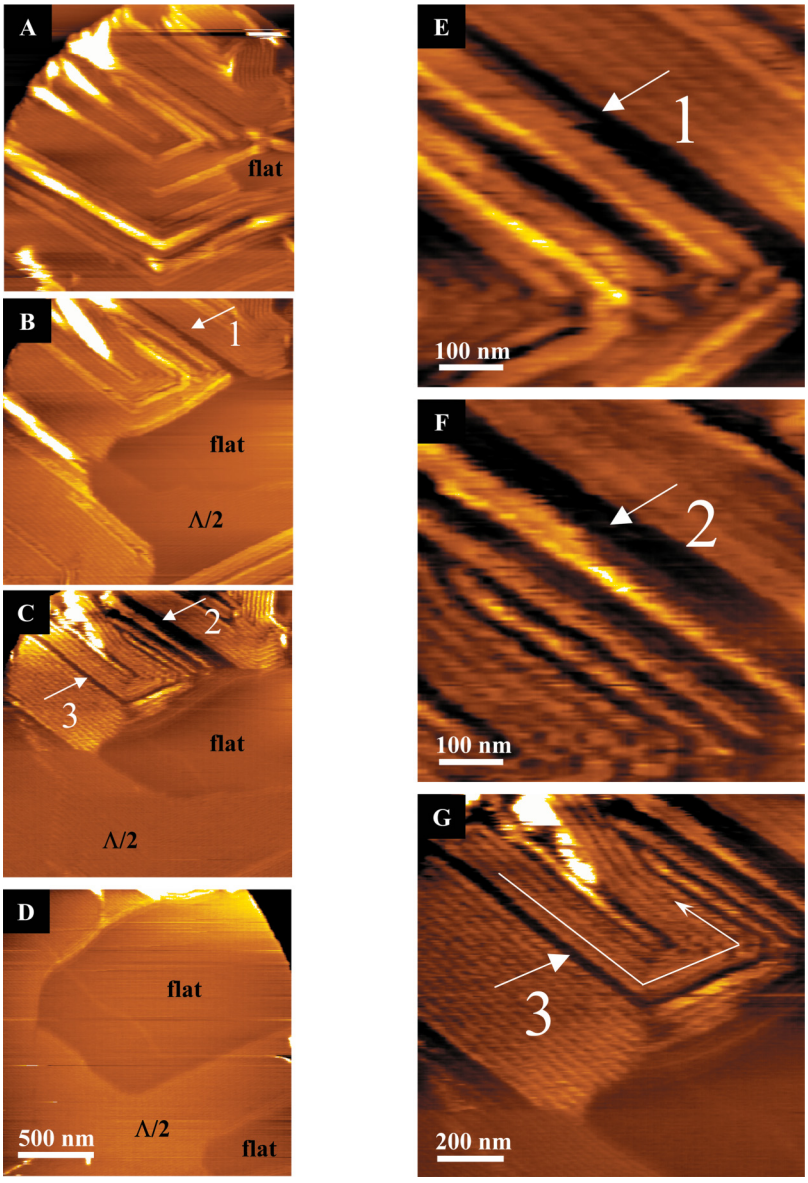

FIGURE 3 Ripple disappearance at the pretransition. The DPPC lipid bilayer was cooled from 37°C to 32°C and the disappearance of the ripples was monitored. A flat region was first observed as shown in *A*. This region grew larger as more ripples disappeared as seen in *B–D*. In *A–D*, it is also seen that the Λ-ripples tend to transform into Λ/2-ripples before completely flattening. *E–F* are magnification images of *B* and *D*, respectively, and demonstrate that ripples disappear very fast in the longitudinal direction once the flattening process of a ripple has been initiated. Arrow 1 in *E* points to a ripple that has partially disappeared. In *F*, this ripple has completely disappeared and the adjacent ripple is now in the process of disappearing as indicated by arrow 2. Arrow 3 in *G* points to a single ripple that has disappeared from within a ripple region, making several turns along its way. The times elapsed after cooling to 32°C are (*A*) 20 min; (*B*) 46 min; (*C*) 49 min; and (*D*) 84 min.

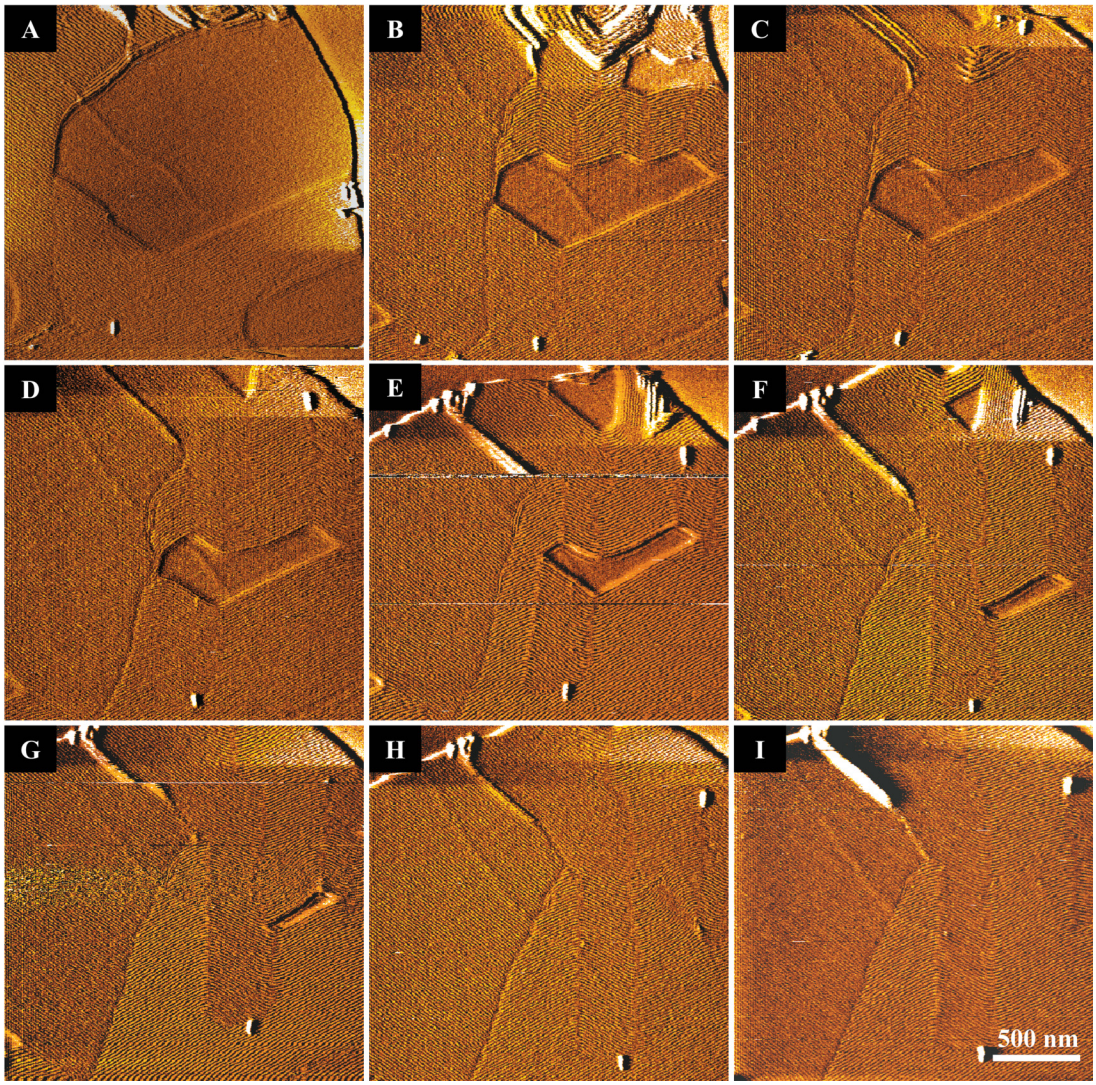

FIGURE 4 Ripple formation at the pretransition. The same lipid bilayer region as shown in Fig. 3 was reheated to 35°C and the re-formation of ripples was monitored. The images are now shown as deflection mode images. (*A*) The same lipid bilayer region shown in height mode in Fig. 3 *D* except that it is here shown in deflection mode. (*B–I*) The lipid bilayer at different times after heating to 35°C. It is seen that ripple formation takes place by the addition of new ripples to the preexisting ripples, which makes the flat regions become progressively smaller with time. The re-formation of ripples happened significantly faster than ripple disappearance. The times elapsed after heating to 35°C are: (*B*) 7 min; (*C*) 10 min; (*D*) 13 min; (*E*) 17 min; (*F*) 21 min; (*G*) 24 min; (*H*) 28 min; and (*I*) 32 min.

of ripples takes place through an intermediate state (Cho et al., 1981). The AFM images strongly support this conclusion, and suggest that the intermediate state is, in fact, the $\Lambda/2$-ripple phase.

The same lipid bilayer island was subsequently reheated to 35°C to study the reappearance of the ripple phase as shown in Fig. 4. The images are now shown in deflection mode, which provides a better visualization of the $\Lambda/2$-ripples. In much the same way as the ripples disappeared one ripple at a time after cooling to 32°C, we observed that ripple formation takes place by the addition of one ripple at a time to the preexisting ripples. This indicates that ripple-growth in the longitudinal direction is a much faster process than the initiation of new ripples in the transverse direction. Another interesting effect to notice is that the ripples clearly tend to change direction at 120° angles, which is particularly evident in Fig. 4 *B*, where a zig-zag pattern is observed just above the flat region. In the following images the ripples in this zig-zag pattern have rearranged to eliminate some of the 120° turns, which indicates that the ripple turns are energetically unfavorable. Furthermore, it should be pointed out that only the $\Lambda/2$-ripples form when entering the ripple-phase temperature region from the gel phase, in accordance with earlier reports (Zasadzinski, 1988; Tenchov et al., 1989; Tenchov, 1991; Yao et al., 1991; Koynova et al., 1996; Katsaras et al., 2000).

In principle, one could imagine two different mechanisms by which the transition from a rippled bilayer to a flat bilayer

can take place. One possible mechanism is by a homogeneous and continuous reduction of the ripple amplitude occurring simultaneously in the entire ripple-phase lipid bilayer. This continuous transformation would be expected if the ripple amplitude depends monotonously on temperature, as Woodward and Zasadzinski (1996) speculated in an earlier study. If, on the other hand, a certain ripple amplitude corresponds to a minimum in the free energy, an abrupt ripple disappearance would be more likely. In this case, the ripples must overcome an energy barrier before reaching the energetically stable planar structure, and one would expect rippled regions to retain the original amplitude until the energy barrier is overcome, whereupon the ripple amplitude would rapidly decrease to zero (or a smaller ripple amplitude corresponding to another local energy minimum). Previous studies on ripple disappearance have shown freeze-fracture electron microscopy snapshots of lipid bilayers cooled below the pretransition but with different results. One study suggests that the ripple phase disappears by an initial dramatic increase in ripple periodicity, which is subsequently followed by the disappearance of a single ripple at a time (Tsuchida et al., 1987). Another study, in accordance with the present article, reports that ripples disappear one ripple at a time without a previous increase in the ripple-periodicity (Kato and Kubo, 1997).

Based on the observations presented above, we conclude that our results do not support the notion of a strongly temperature-dependent amplitude, where the amplitude is close to zero at the pretransition and increases as the main phase transition is approached. Rather, we suggest an abrupt mechanism of ripple formation, where ripple clusters form by nucleation events in different places of the bilayer and subsequently act as sites for further ripple growth.

As a closing remark in relation to one-component lipid bilayers, we point out that the temperature range for ripple formation and disappearance that we have observed in the supported double bilayers (32–35°C) is in good agreement with differential scanning calorimetry measurements on lipid vesicle suspensions (Parente and Lentz, 1984; Tenchov et al., 1989). We therefore conclude that supported double bilayers are unperturbed by the solid support. It might be argued, however, that the scanning of the lipid bilayers with the AFM tip introduces a slight perturbation of the system, but we find it highly reassuring that the ripple phase reforms at 35°C despite repeated scanning.

Ripple phases in two-component lipid bilayers: Heating of a 7:3 DMPC-DSPC lipid mixture

The preceding paragraphs have described the structure of the ripple phase in one-component DPPC lipid bilayers. Also, the structural changes that occur when crossing the pretransition in both the cooling and the heating direction were addressed. We now switch to two-component DMPC-DSPC lipid mixtures. In previous work, we have shown for such mixtures that the ripple phase creates an anisotropic line tension in the ripple-phase/fluid-phase coexistence region, which results in the formation of straight-edged domains with characteristic 60° and 120° angles (Leidy et al., 2002). In the following, we present images of a 7:3 DMPC-DSPC lipid bilayer that is heated from the ripple phase, across the *solidus* phase line, and into the ripple phase/fluid phase coexistence region. The images reveal several important events responsible for the characteristic appearance of the lipid bilayer in the phase coexistence region. These events are related to various properties of the ripple phase and will be discussed individually in the following paragraphs.

Interconversion of ripples

The 7:3 DMPC-DSPC-supported double bilayer was prepared by incubating small unilamellar vesicles on freshly cleaved mica at 24°C. At this temperature, the only type of ripples that were observed were metastable Λ-ripples (data not shown). When the temperature was raised, however, an interconversion of the metastable Λ-ripples to the stable Λ/2-ripples took place. The interconversion was first observed at 26°C as a small region of Λ/2-ripples that appeared inside the Λ-ripple phase. This region started out as a small domain with an almost rectangular shape having ripples running in the direction of the longer side of the rectangle. As the temperature was maintained at 26–27°C, the domain grew in size and attained an elongated rodlike appearance, due to the fact that growth proceeded faster in the direction of the ripples as compared to the transverse direction. Fig. 5 shows a fraction of the Λ/2-ripple domain as well as the adjoining Λ-ripples from which the Λ/2-ripple domain emerged. The different ripple types and ripple directions have been outlined in the deflection mode image (Fig. 5 *B*), which shows the ripples more clearly than the height mode image in Fig. 5 *A*. It is noteworthy that the Λ/2 ripples are unidirectional and all oriented vertically in the image. In contrast, the adjoining Λ-ripples are not unidirectional but appear as regions each having their own ripple direction, as indicated in Fig. 5 *B*. In the height mode image (Fig. 5 *A*), the Λ/2-ripple domain is observed as the darker region on the left side of the image and the Λ-ripples correspond to the brighter area on the right. The Λ/2-ripple domain thus appears to be lower than the adjoining Λ-ripples as indicated by the darker colors of the Λ/2-region. However, this appearance is likely to be an artifact arising from the finite radius of the AFM tip, which prevents it from reaching the bottom of the narrow ripple valleys. In such cases where the tip images the ripple peaks correctly although it is unable to reach the ripple valleys, an apparent height difference might arise from a difference in ripple amplitudes, whereas the average bilayer height, in reality, is the same. In addition to the different ripple domains, some rounded domains are also observed. These rounded features reflect lipid domains that form in the bottom bilayer, and are visible as imprints in the top bilayer (Leidy et al., 2002). The domains in the bottom bilayer are

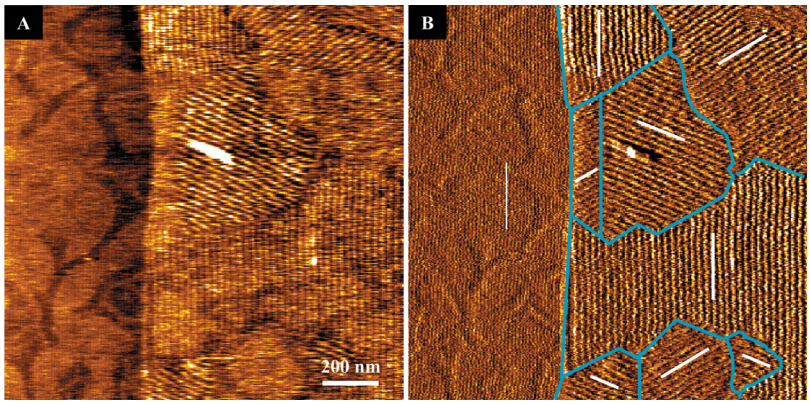

FIGURE 5 Height mode (*A*) and deflection mode (*B*) images of the interfacial region between a Λ/2-ripple domain and several Λ-ripple domains in a 7:3 DMPC-DSPC lipid bilayer at 26.0°C. The Λ/2-ripple domain emerged from within a region of Λ-ripples by an interconversion of Λ-ripples to Λ/2-ripples. The Λ/2-ripple domain is visible as the darker region on the left in the height mode image (*A*) and as the short-wavelength ripples on the left in the deflection mode image (*B*). Whereas the Λ/2-ripples were all oriented in the same direction, the Λ-ripples were present as a number of different regions that each had their own ripple direction. The different ripple regions and directions have been outlined in *B*. The rounded structures that are also seen, and are particularly visible in the Λ/2-ripple domain, correspond to domains in the first bilayer in close contact with the mica support.

notably different due to the influence of the mica support, which inhibits ripple-phase formation. Similar domain structures have been reported in AFM studies of DMPC-DSPC supported single bilayers (Giocondi et al., 2001).

Interfacial melting at the *solidus* phase line

Fig. 6, *A* and *B*, shows a larger view of the Λ/2-ripple domain surrounded by Λ-ripples. The Λ/2-ripple domain is visible as the darker elongated region in the height mode image (Fig. 6 *A*), whereas the surrounding brighter area corresponds to Λ-ripples, which are regions that each have their own ripple direction. The different Λ-ripple directions are indicated by white bars in Fig. 6 *B*. Because of the large scan size of Fig. 6, the resolution is poorer than in Fig. 5, and for this reason it was only possible to determine the ripple direction on the right-hand side of the image.

Fig. 6, *C* and *D*, shows the same bilayer region as in Fig. 6, *A* and *B*, after a small temperature increase of 0.5°C. The temperature is now 27.5°C, which is close to the *solidus* phase line for the DMPC-DSPC mixture. Melting is observed at the interface between the Λ/2-ripple domain and the surrounding

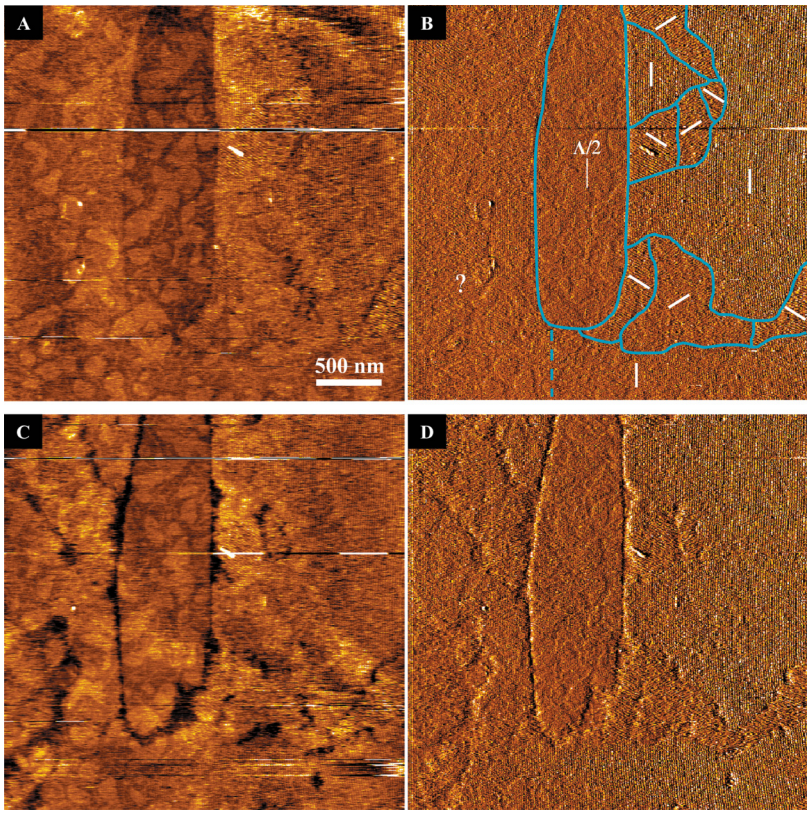

FIGURE 6 Interfacial melting at the *solidus* phase line. (*A*) Height mode image of the Λ/2-ripple domain surrounded by Λ-ripples. (*B*) Corresponding deflection mode image. The Λ/2-ripple domain as well as some of the surrounding Λ-ripple domains are outlined. It was only possible to discern the Λ-ripple domains on the right-hand side of the image. The temperature was 27.0°C. (*C*) Same region after a small temperature increase to 27.5°C. The lipid bilayer has started to melt at the interface between the Λ/2-ripple domain and the surrounding Λ-ripple regions. Furthermore, melting is observed in several places of the Λ-ripple domains. A comparison of the melted areas to the domains outlined in *B* reveals that the domain boundaries act as initiation sites for melting. (*D*) Corresponding deflection mode image.

Λ-ripple region. This is observed as a dark area surrounding the Λ/2-ripple domain. Melting has predominantly occurred at the points where the Λ/2-ripple domain is bordered by Λ-ripples of a different ripple orientation. In addition, numerous small melted regions are observed in various places of the Λ-region whereas no melting has taken place inside the Λ/2-domain. By comparing the ripple directions outlined in Fig. 6 *B* to the melted regions in Fig. 6 *C* it is evident that melting is initiated at the sites where the ripples change orientation. These observations therefore imply that both the interfacial region between Λ/2-ripples and Λ-ripples as well as regions where ripples change direction represent areas of lower stability and therefore act as starting points of melting. A straightforward explanation is that these regions have a higher degree of lipid disorder due to packing constraints as earlier suggested (Kapitza et al., 1984; Mouritsen and Zuckermann, 1987).

Although melting occurs around the Λ/2-domain, no melting is observed inside of the domain. We do not find this surprising for the following reasons. First of all, the Λ/2-domain is a single domain having only one ripple direction and no areas where different ripple directions meet, which can serve as starting points for melting. Secondly, Λ/2-ripples are considered the stable ripple phase, and are therefore expected to melt at a slightly higher temperature than the Λ-ripple phase.

Domain growth, further melting, and structural rearrangements

Fig. 7, *A–D* shows later stages of the melting process. Interestingly, after heating the bilayer to 28°C, the Λ/2-ripple-phase domain continues to grow by recruiting lipids from the surrounding fluid phase, while at the same time the Λ-region shrinks as melting proceeds. This observation is a further indication that the Λ/2-ripple phase is more stable than the Λ-ripple phase. In Fig. 7 *B* the bilayer is further heated to 29°C and melting has now initiated inside of the Λ/2-domain. It is interesting to observe that the melted regions take on remarkable elongated shapes that are parallel with the ripple direction. This results from the fact that the ripples favor this direction of melting. Fig. 7 *C* shows the bilayer at 30.0°C, where the melted regions inside the ripple-phase domain have grown further in size.

Fig. 7 *D* shows a deflection mode image at 32.5°C at a later point in time. The shape of the domain has now drastically changed and sharp 60° and 120° angles have developed. We speculate that the reason for this structural rearrangement is related to a rupture of the ripple phase structure surrounding the fluid phase domain, due to an increase in lateral stress in the ripple-phase domain that develops as the melted regions grow. It is well-known that lipid bilayers expand laterally during melting. Therefore, we expect that the melted regions

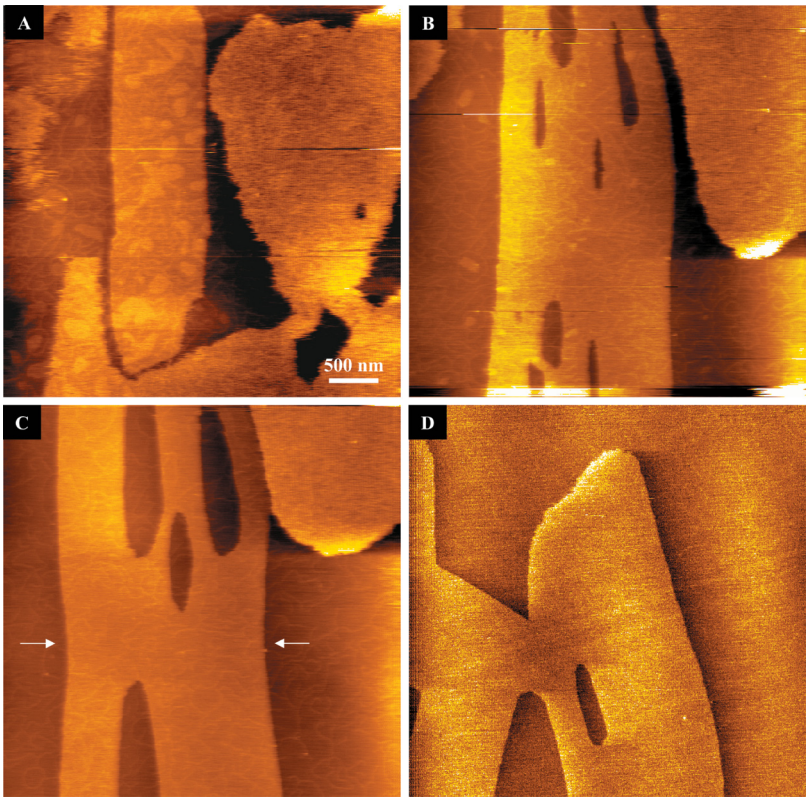

FIGURE 7 Further melting, domain growth, and structural rearrangements. (*A*) Same bilayer region as in Fig. 6. Upon further heating, the Λ-ripple regions continued to melt, while the Λ/2-ripple domain grew larger. The Λ/2-ripple domain is visible in the center of the image. The temperature is 28.0°C. (*B*) Upon further heating, melted regions appeared inside of the Λ/2-ripple domain. The melted domains attained elongated shapes because of the anisotropic nature of the ripple phase. The temperature is 29.0°C. (*C*) The melted regions inside the Λ/2-ripple domain have grown. The temperature is 30.0°C. (*D*) A dramatic change in the domain shape took place and characteristic 60° and 120° angles were observed. The temperature is 32.5°C.

inside the ripple-phase domain have a tendency to expand and thereby create a pressure against the neighboring ripple-phase lipids. That this indeed occurs is supported by Fig. 7 *C*, which shows that the ripple-phase domain has developed a waistlike shape in the middle section (marked by the *arrows*) where no melted domains are present, whereas the top and the bottom parts where fluid domains are emerging are clearly broader. At the same time that the melted domains expand laterally, the ripples prefer to keep in a straight-line orientation. Consequently, the lateral pressure inside the ripple-phase domain becomes larger than the pressure outside the domain where the fluid-phase lipids are able to expand freely. When this pressure becomes large enough, a branch of ripple-phase lipids will break loose. The specific angles that form after rupture are most likely derived from the fact that the branches assume the most stable orientations with respect to their points of attachment, and the nature of the ripple phase makes 60° and 120° angles the preferred orientations.

CONCLUSION

Our temperature-controlled AFM images have visualized the structure and kinetics of ripple phases in one- and two-component lipid bilayers and provided several examples of the anisotropic nature of ripple phases. In one-component bilayers, the anisotropy was manifested by the formation of ripples at the pretransition, which took place by adding a single ripple at a time to the preexisting ripples. Likewise, the ripples disappeared one by one upon cooling a ripple-phase lipid bilayer into the gel phase, clearly showing that both the formation and disappearance of ripples happen much faster in the longitudinal direction than in the transverse direction of the ripples. Three different ripple types were observed in DPPC lipid bilayers when cooled from the fluid-phase to the ripple-phase temperature range. In addition to the stable and metastable ripple phases that are commonly observed, a third ripple type of approximately double the dimensions of the metastable ripple phase appeared. The amplitudes of the three ripple types were estimated to be $\geq$12 Å, $\geq$50 Å, and $\geq$110 Å, which should be considered lower-limit values. In the two-component DMPC-DSPC system, the ripple phase favored domain growth along the ripple direction and dictated the creation of 60° and 120° angles of the ripple-phase domains. Close to the *solidus* phase line, an interconversion of Λ-ripples to $\Lambda/2$ ripples was observed, and upon further heating the Λ-ripples melted before the $\Lambda/2$-ripples, confirming that the $\Lambda/2$-ripples are the thermodynamically stable ripple variety. Onset of melting was observed at sites where the ripples change direction and at the interface between $\Lambda/2$ and Λ-ripples. A common conclusion that can be drawn from the present study is that the ripple phase is characterized by long-range two-dimensional hexagonal order of the phospholipids, and is responsible for distorting the underlying hexagonal lattice in a way that has important consequences for the melting behavior of ripple-phase lipid bilayers.

This work was supported by the Hasselblad Foundation, the Apoteker Foundation of 1991, and by grant N660001-00-C-8048 from the Defense Advanced Research Projects Agency to J.H.C. The MEMPHYS-Center for Biomembrane Physics is supported by the Danish National Research Foundation.

REFERENCES

Bagatolli, L. A., and E. Gratton. 2000. A correlation between lipid domain shape and binary phospholipid mixture composition in free standing bilayers: a two-photon fluorescence microscopy study. *Biophys. J.* 79: 434–447.

Carlson, J. M., and J. P. Sethna. 1987. Theory of the ripple phase in hydrated phospholipid bilayers. *Phys. Rev. A.* 36:3359–3374.

Cho, K. C., C. L. Choy, and K. Young. 1981. Kinetics of the pretransition of synthetic phospholipids: a calorimetric study. *Biochim. Biophys. Acta.* 663:14–21.

Copeland, B. R., and H. M. McConnell. 1980. The rippled structure in bilayer membranes of phosphatidylcholine and binary mixtures of phosphatidylcholine and cholesterol. *Biochim. Biophys. Acta.* 599:95–109.

Czajkowsky, D. M., C. Huang, and Z. F. Shao. 1995. Ripple phase in asymmetric unilamellar bilayers with saturated and unsaturated phospholipids. *Biochemistry.* 34:12501–12505.

Doniach, S. 1979. A thermodynamic model for the monoclinic (ripple) phase of hydrated phospholipid bilayers. *J. Chem. Phys.* 70:4587–4596.

Fang, Y., and J. Yang. 1996. Role of the bilayer-bilayer interaction on the ripple structure of supported bilayers in solution. *J. Phys. Chem.* 100: 15614–15619.

Fluck, D. J., A. F. Henson, and D. Chapman. 1969. The structure of dilute lecithin-water systems revealed by freeze-etching and electron microscopy. *J. Ultrastruct. Res.* 29:416–429.

Giocondi, M. C., L. Pacheco, P. E. Milhiet, and C. Le Grimellec. 2001. Temperature dependence of the topology of supported dimyristoyl-distearoyl phosphatidylcholine bilayers. *Ultramicroscopy.* 86:151–157.

Heimburg, T. 2000. A model for the lipid pretransition: coupling of ripple formation with the chain-melting transition. *Biophys. J.* 78:1154–1165.

Hicks, A., M. Dinda, and M. A. Singer. 1987. The ripple phase of phosphatidylcholines—effect of chain-length and cholesterol. *Biochim. Biophys. Acta.* 903:177–185.

Janiak, M. J., D. M. Small, and G. G. Shipley. 1979. Temperature and compositional dependence of the structure of hydrated dimyristoyl lecithin. *J. Biol. Chem.* 254:6068–6078.

Kapitza, H. G., D. A. Rüppel, H.-J. Galla, and E. Sackmann. 1984. Lateral diffusion of lipids and glycophorin in solid phosphatidylcholine bilayers. The role of structural defects. *Biophys. J.* 45:577–587.

Kato, S., and T. Kubo. 1997. Relaxation process after the cooling jump across the pretransition of dipalmitoylphosphatidylcholine bilayers. *Chem. Phys. Lipids.* 90:31–44.

Katsaras, J., S. Tristram-Nagle, Y. Liu, R. L. Headrick, E. Fontes, P. C. Mason, and J. F. Nagle. 2000. Clarification of the ripple phase of lecithin bilayers using fully hydrated, aligned samples. *Phys. Rev. E.* 61:5668–5677.

Kirchner, S., and G. Cevc. 1994. On the origin of thermal $L(\beta')$–$P(\beta')$ pretransition in the lamellar phospholipid membranes. *Eur. Phys. Lett.* 28:31–36.

Korlach, J., P. Schwille, W. W. Webb, and G. W. Feigenson. 1999. Characterization of lipid bilayer phases by confocal microscopy and fluorescence correlation spectroscopy. *Proc. Natl. Acad. Sci. USA.* 96: 8461–8466.

Koynova, R., A. Koumanov, and B. Tenchov. 1996. Metastable rippled gel phase in saturated phosphatidylcholines: calorimetric and densitometric characterization. *Biochim. Biophys. Acta.* 1285:101–108.

Krbecek, R., C. Gebhardt, C. Gruler, and E. Sackmann. 1979. Three dimensional microscopic surface profiles of membranes reconstituted from freeze etching electron micrographs. *Biochim. Biophys. Acta*. 554: 1–22.

Leidy, C., T. Kaasgaard, J. H. Crowe, O. G. Mouritsen, and K. Jørgensen. 2002. Ripples and the formation of anisotropic lipid domains: imaging two-component supported double bilayers by atomic force microscopy. *Biophys. J*. 83:2625–2633.

Lewis, R. N. A. H., N. Mak, and R. N. McElhaney. 1987. A differential scanning calorimetric study of the thermotropic phase behavior of model membranes composed of phosphatidylcholines containing linear saturated fatty acyl chains. *Biochemistry*. 26:6118–6126.

Lubensky, T. C., and F. C. Mackintosh. 1993. Theory of ripple phases of lipid bilayers. *Phys. Rev. Lett*. 71:1565–1568.

Matuoka, S., S. Kato, and I. Hatta. 1994. Temperature-change of the ripple structure in fully hydrated dimyristoylphosphatidylcholine cholesterol multibilayers. *Biophys. J*. 67:728–736.

Meyer, H. W. 1996. Pretransition-ripples in bilayers of dipalmitoylphosphatidylcholine: undulation or periodic segments? A freeze-fracture study. *Biochim. Biophys. Acta*. 1302:138–144.

Mortensen, K., W. Pfeiffer, E. Sackmann, and W. Knoll. 1988. Structural properties of a phosphatidylcholine-cholesterol system as studied by small-angle, neutron-scattering: ripple structure and phase diagram. *Biochim. Biophys. Acta*. 945:221–245.

Mou, J. X., J. Yang, and Z. F. Shao. 1994. Tris(hydroxymethyl)aminomethane (C4H11NO3) induced a ripple phase in supported unilamellar phospholipid bilayers. *Biochemistry*. 33:4439–4443.

Mouritsen, O. G., and M. J. Zuckermann. 1987. Model of interfacial melting. *Phys. Rev. Lett*. 58:389–392.

Parente, R. A., and B. R. Lentz. 1984. Phase behavior of large unilamellar vesicles composed of synthetic phospholipids. *Biochemistry*. 23:2353–2362.

Rappolt, M., G. Pabst, G. Rapp, M. Kriechbaum, H. Amenitsch, C. Krenn, S. Bernstorff, and P. Laggner. 2000. New evidence for gel-liquid crystalline phase coexistence in the ripple phase of phosphatidylcholines. *Eur. Biophys. J*. 29:125–133.

Rappolt, M., and G. Rapp. 1996. Structure of the stable and metastable ripple phase of dipalmitoylphosphatidylcholine. *Eur. Biophys. J*. 24:381–386.

Rüppel, D., and E. Sackmann. 1983. On defects in different phases of two-dimensional lipid bilayers. *J. Phys*. 44:1025–1034.

Stamatoff, J., B. Feuer, H. J. Guggenheim, G. Tellez, and T. Yamane. 1982. Amplitude of rippling in the P'_β phase of dipalmitoylphosphatidylcholine bilayers. *Biophys. J*. 38:217–226.

Sun, W.-J., S. Tristram-Nagle, R. M. Suter, and J. F. Nagle. 1996. Structure of the ripple phase in lecithin bilayers. *Proc. Natl. Acad. Sci. USA*. 93: 7008–7012.

Tenchov, B. 1991. On the reversibility of the phase transitions in lipid-water systems. *Chem. Phys. Lipids*. 57:165–177.

Tenchov, B. G., H. Yao, and I. Hatta. 1989. Time-resolved x-ray diffraction and calorimetric studies at low scan rates. 1. Fully hydrated dipalmitoylphosphatidylcholine (DPPC) and DPPC/water ethanol phases. *Biophys. J*. 56:757–768.

Tsuchida, K., I. Hatta, S. Imaizumi, K. Ohki, and Y. Nozawa. 1985. Kinetics near the pretransition of a multilamellar phospholipid studied by ESR. *Biochim. Biophys. Acta*. 812:249–254.

Tsuchida, K., K. Ohki, T. Sekiya, Y. Nozawa, and I. Hatta. 1987. Dynamics of appearance and disappearance of the ripple structure in multilamellar liposomes of dipalmitoylphosphatidylcholine. *Biochim. Biophys. Acta*. 898:53–58.

Ververgaert, P. H. J., A. J. Verkleij, P. F. Elbers, and L. L. M. van Deenen. 1973. Analysis of the crystallization process in lecithin liposomes: a freeze-etch study. *Biochim. Biophys. Acta*. 311:320–329.

Woodward, J. T., and J. A. Zasadzinski. 1996. Amplitude, wave form, and temperature dependence of bilayer ripples in the P'_β phase. *Phys. Rev. E*. 53:R3044–R3047.

Yao, H., S. Matuoka, B. Tenchov, and I. Hatta. 1991. Metastable ripple phase of fully hydrated dipalmitoylphosphatidylcholine as studied by small-angle x-ray scattering. *Biophys. J*. 59:252–255.

Zasadzinski, J. A. N. 1988. Effect of stereo configuration on ripple phases (P'_β) of dipalmitoylphosphatidylcholine. *Biochim. Biophys. Acta*. 946: 235–243.